Level Crossing Rate and Average Fade Duration in MIMO Mobile Fading Channels

Ali Abdi, Chunjun Gao, Alexander M. Haimovich

Dept. of Elec. and Comp. Eng., New Jersey Institute of Technology, Newark, NJ 07102, USA

Emails: ali.abdi@njit.edu, cxg9074@njit.edu, haimovich@adm.njit.edu

***Abstract* – In this paper, important dynamic characteristics of MIMO mobile fading channels such as the level crossing rate (LCR) and average fade durations (AFD) are studied. Depending on the application, either a scalar crossing approach or a vector crossing approach is taken, and appropriate definitions for LCR and AFD in MIMO channels are provided. The more general concept of average stay duration (ASD) is also defined. Closed-from solutions for *scalar* MIMO LCR and *vector* MIMO ASD are presented, and illustrated via numerical examples. Finally, the utility of the new definitions and results, when applied to adaptive modulation in MIMO channels, Markov modeling, and the block fading approximation of MIMO channels are discussed as well.**

I. Introduction

In mobile communications with time-selective fading, the level crossing rate (LCR), how often the signal crosses a certain threshold, is an important dynamic characteristic of the channel. The average fade duration (AFD), how long the signal stays below a given threshold, can be calculated from LCR and appears in a variety of applications. Choosing the frame length of coded packetized systems [1] and also interleaver optimization, to efficiently combat the burst of errors due to long fades, need the AFD information [2] [3]. In adaptive modulation schemes, the average time that a particular constellation is continuously used is related to AFD [4]. Average outage duration in multiuser cellular systems [5] [6], where interference from other users restricts the performance, is another close relative of AFD. Throughput (efficiency) of communication protocols such as automatic repeat request (ARQ) schemes can be estimated using AFD [7]. The transition probabilities between different states of a Markov model for fading channels has been calculated based on LCR at different levels [8].

In recent years, wireless communication over multiple-input multiple-output (MIMO) fading channels has become an active research area, specially due the very high data transmission rates that can be achieved in multi-antenna systems. Clearly, efficient communication over MIMO mobile fading channels requires a basic understanding of the statistical structure of such random channels, which could be different from the traditional single-input single-output (SISO) and single-input multiple-output (SIMO) channels. Some important characteristics of MIMO channels, such as space-time correlations in macrocells [9] and space-time-frequency correlations in macrocells [10], have been explored so far. However, to the best of our knowledge, the concepts of LCR and AFD for MIMO fading channels have not yet been defined and analyzed.

More specifically, most of the LCR- and AFD-related research has been carried out in the context of SISO systems. The recent works on LCR and AFD for receive diversity combiners [11] [12] [13] [14], which eventually boil down to the crossing theory of a scalar process, appear in MIMO channels, as we will see in the sequel. However, in general, for an *M*-transmit *N*-receive multiantenna system, the *joint* dynamic behavior of *MN* correlated random signals is of interest (which has not been addressed in the literature). This requires a multidimensional approach to LCR and AFD problems.

To show the utility of the theoretical results derived in this paper, we briefly discuss adaptive modulation, Markov modeling, the block fading model, and the concept of vector AFD in MIMO systems. In the first two cases we have a scalar crossing problem, whereas the last two require a vector crossing approach.

The rest of this paper is organized as follows. In Sections II and III, the scalar and vector crossing problems in MIMO systems are discussed, respectively. Concluding remarks are given in Section IV.

II. Scalar Crossing in MIMO Systems

In this section, first we present the mathematical formulation of the problem and its solution, followed by a numerical example. Then we highlight the applications.

A. Mathematical Formulation

Consider a time-selective narrowband $M \times N$ channel, with *MN* complex Gaussian processes, correlated in both space and time, and corrupted by a spatio-temporal white Gaussian noise. Obviously, depending on the presence or absence of line-of-sight (LOS), the envelope of subchannels could be Rice or Rayleigh, respectively. The instantaneous received signal-to-noise ratio (SNR) per symbol over the subchannel from the *p*-th transmitter to the *l*-th receiver is proportional to $|h_{lp}(t)|^2$, assuming perfect channel estimation at the receiver. The total instantaneous received SNR per symbol, $\gamma(t)$, is therefore proportional to $\sum_{l,p}|h_{lp}(t)|^2$, and is a useful measure for Markov modeling of diversity systems [15], MIMO channel characterization [16] [17], and design of MIMO systems [18] [19].

Now we want to determine the average stay duration (ASD) of $\gamma(t)$ within the region $[\gamma_1, \gamma_2]$, $\mathrm{ASD}\{\gamma(t),[\gamma_1,\gamma_2]\}$, defined as the average time over which $\gamma_1 \le \gamma(t) \le \gamma_2$. The concept of ASD is applicable to both scalar processes such as $\gamma(t)$, as well as vector processes, discussed later, and includes AFD as the special case where $\gamma_1 = -\infty$. Similar to AFD, the ASD of $\gamma(t)$ within the region $[\gamma_1, \gamma_2]$ can be calculated according to $\mathrm{ASD}\{\gamma(t),[\gamma_1,\gamma_2]\} = \Pr[\gamma_1 \le \gamma \le \gamma_2] / \mathrm{ICR}\{\gamma(t),[\gamma_1,\gamma_2]\}$, where Pr[.] is the probability and the denominator is the incrossing rate (ICR), i.e., the average number of times that $\gamma(t)$ crosses one of the two borders and enters the region $[\gamma_1, \gamma_2]$. The numerator can be calculated via the Euler method [20]. For the denominator we use the result of [21].

Specifically, let $x(t) = \sum_{i=1}^{J} u_i^2(t)$, where $u_i(t)$ s are correlated nonzero mean real Gaussian processes. Also let $\boldsymbol{u} = [u_1 u_2 ... u_J]^T$ and $\boldsymbol{u}' = [u_1' u_2' ... u_J']^T$, where prime denotes differentiation with respect to time *t* and ^{T} is the transpose operator. The mean vector and the covariance matrix of $[\boldsymbol{u}^T \boldsymbol{u}'^T]^T$ are given by

$$[\boldsymbol{\eta}^T \mathbf{0}^T]^T, \quad \boldsymbol{\Sigma} = \begin{bmatrix} \boldsymbol{\Sigma}_{11} & \boldsymbol{\Sigma}_{12} \\ \boldsymbol{\Sigma}_{21} & \boldsymbol{\Sigma}_{22} \end{bmatrix}, \tag{1}$$

where $\boldsymbol{\eta}$ is a $J\times 1$ vector, $\mathbf{0}$ is a $J\times 1$ zero vector, and $\boldsymbol{\Sigma}_{21}=\boldsymbol{\Sigma}_{12}^{T}$. We also need the following transformations

$$\begin{aligned}
&u_1=\sqrt{x}\cos(\theta_1)...\cos(\theta_{J-1}),\\
&u_2=\sqrt{x}\cos(\theta_1)...\cos(\theta_{J-2})\sin(\theta_{J-1}),\\
&\vdots\\
&u_i=\sqrt{x}\cos(\theta_1)...\cos(\theta_{J-i})\sin(\theta_{J-i+1}),\\
&\vdots\\
&u_J=\sqrt{x}\sin(\theta_1),
\end{aligned}\tag{2}$$

where $\theta_i\in[-\pi/2,\pi/2)$, $i=1,2,...,J-2$, and $\theta_{J-1}\in[0,2\pi)$. Then the upcrossing rate (UCR) of $x(t)$ with respect to the threshold x_0 can be written as [21]

$$\begin{aligned}
&\mathrm{UCR}\{x(t),x_0\}=(2\pi)^{-(J+1)/2}[\det(\boldsymbol{\Sigma}_{11})]^{-1/2}x_0^{(J-2)/2}\\
&\int_{-\pi/2}^{\pi/2}...\int_{-\pi/2}^{\pi/2}\int_{0}^{2\pi}\left\{\sigma\exp\left(\frac{-\vartheta^2}{2\sigma^2}\right)+(2\pi)^{1/2}\vartheta\left[1-\Phi\left(\frac{-\vartheta}{\sigma}\right)\right]\right\}\\
&\qquad\times\exp\left[-\tfrac{1}{2}A(x_0,\theta_1,...,\theta_{J-1})\right]B(\theta_1,...,\theta_{J-2})\,d\theta_1...d\theta_{J-1},
\end{aligned}\tag{3}$$

where det(.) is the determinant and

$$\begin{aligned}
&\sigma^2=4\boldsymbol{u}^T(\boldsymbol{\Sigma}_{22}-\boldsymbol{\Sigma}_{21}\boldsymbol{\Sigma}_{11}^{-1}\boldsymbol{\Sigma}_{12})\boldsymbol{u},\\
&\vartheta=2\boldsymbol{u}^T\boldsymbol{\Sigma}_{21}\boldsymbol{\Sigma}_{11}^{-1}(\boldsymbol{u}-\boldsymbol{\eta}),\\
&\Phi(y)=(2\pi)^{-1/2}\int_{-\infty}^{y}\exp(-z^2/2)dz,\\
&A(x_0,\theta_1,...,\theta_{J-1})=(\boldsymbol{u}-\boldsymbol{\eta})^T\boldsymbol{\Sigma}_{11}^{-1}(\boldsymbol{u}-\boldsymbol{\eta}),\\
&B(\theta_1,...,\theta_{J-2})=\tfrac{1}{2}\cos^{J-2}(\theta_1)\cos^{J-3}(\theta_2)...\cos(\theta_{J-2}).
\end{aligned}\tag{4}$$

When $u_i(t)$ s are identically-distributed and correlated zero-mean real Gaussian processes, a compact form is given in [22] for $\mathrm{UCR}\{x(t),x_0\}$. Note that $\mathrm{DCR}\{x(t),x_0\}=\mathrm{UCR}\{x(t),x_0\}$, where DCR stands for the downcrossing rate.

Obviously $\mathrm{ICR}\{\gamma(t),[\gamma_1,\gamma_2]\}=\mathrm{UCR}\{\gamma(t),\gamma_1\}+\mathrm{DCR}\{\gamma(t),\gamma_2\}$. In an $M\times N$ MIMO system, we have $J=2MN$. Therefore, to calculate $\mathrm{ICR}\{\gamma(t),[\gamma_1,\gamma_2]\}$, two $(2MN-1)$-fold finite-range integrals need to be calculated. This could be very cumbersome even for a simple 2×2 system, which entails two seven-fold integrals. We are developing a technique which has much less computational complexity, and will be reported in another paper.

B. Numerical Example

Consider a 2×1 Rayleigh channel, i.e., $M=2$ and $N=1$. Then total instantaneous received SNR per symbol is given by $\gamma(t)=(E_{av}/N_0)(|h_{11}(t)|^2+|h_{12}(t)|^2)$, where E_s/N_0 is the average SNR per symbol. Let $E[|h_{11}(t)|^2]=E[|h_{12}(t)|^2]=1$. Therefore the average received SNR per symbol over each subchannel is given by $\overline{\gamma}_{11}=E_s/N_0$. Now we rewrite the total instantaneous received SNR per symbol as $\gamma(t)=\overline{\gamma}_{11}(|h_{11}(t)|^2+|h_{12}(t)|^2)$. We also define the temporal autocorrelation $\rho_{11,11}(\tau)=E[h_{11}(t)h_{11}^*(t+\tau)]=\rho_{12,12}(\tau)$ and spatio-temporal crosscorrelation $\rho_{11,12}(\tau)=E[h_{11}(t)h_{12}^*(t+\tau)]$, where * is the complex conjugate.

To calculate the AFD of $\gamma(t)$ below the threshold γ_{th}, $\mathrm{AFD}\{\gamma(t),\gamma_{th}\}$, we need to calculate $\Pr[\gamma\le\gamma_{th}]$ and $\mathrm{DCR}\{\gamma(t),\gamma_{th}\}$. For the former we use the result given in [23], p. 368

$$\begin{aligned}
\Pr[\gamma\le\gamma_{th}]=1-&(2|\zeta|)^{-1}\Big[(1+|\zeta|)\exp\Big\{-\gamma_{th}\Big[\overline{\gamma}_{11}(1+|\zeta|)\Big]^{-1}\Big\}\\
&-(1-|\zeta|)\exp\Big\{-\gamma_{th}\Big[\overline{\gamma}_{11}(1-|\zeta|)\Big]^{-1}\Big\}\Big],
\end{aligned}\tag{5}$$

where $\zeta=\rho_{11,12}(0)$, and for the latter we compute (3), numerically.

To compute (3), we define $u_i(t)$ s such that $h_{11}(t)=u_1(t)+ju_2(t)$ and $h_{12}(t)=u_3(t)+ju_4(t)$, in which $j^2=-1$. For mathematical convenience, we define the vector $\boldsymbol{u}$ as $\boldsymbol{u}=[u_1\,u_3\,u_2\,u_4]^T$. Such a definition makes $\boldsymbol{\Sigma}_{11}$, $\boldsymbol{\Sigma}_{12}$, and $\boldsymbol{\Sigma}_{22}$ in (1), block matrices, as we will see later. Due to Rayleigh fading $\boldsymbol{\eta}=E[\boldsymbol{u}]=\mathbf{0}$. To build the covariance matrix in (1), we need to express $E[u_i(t)u_k(t+\tau)]$, $i,k=1,...,4$, in terms of $\rho_{11,11}(\tau)$ and $\rho_{11,12}(\tau)$. It is easy to verify that

$$\begin{aligned}
&E[u_i(t)u_i(t+\tau)]=\tfrac{1}{2}\mathrm{Re}[\rho_{11,11}(\tau)],\ i=1,...,4,\\
&E[u_1(t)u_2(t+\tau)]=E[u_3(t)u_4(t+\tau)]=\tfrac{-1}{2}\mathrm{Im}[\rho_{11,11}(\tau)],\\
&E[u_1(t)u_3(t+\tau)]=E[u_2(t)u_4(t+\tau)]=\tfrac{1}{2}\mathrm{Re}[\rho_{11,12}(\tau)],\\
&E[u_1(t)u_4(t+\tau)]=-E[u_2(t)u_3(t+\tau)]=\tfrac{-1}{2}\mathrm{Im}[\rho_{11,12}(\tau)],
\end{aligned}\tag{6}$$

where Re[.] and Im[.] give the real and imaginary parts, respectively. In deriving the equations in (6), we have considered the class of widely-used rotation invariant [25] (also called proper [26]) complex random vectors and processes. This translates into $E[h_{11}^2(t)]=E[h_{12}^2(t)]=E[h_{11}(t)h_{12}(t)]=0$.

Based on (6), it is easy to construct $\boldsymbol{\Sigma}_{11}$, which is a symmetric matrix. To calculate the elements of the other two covariance matrices in (1), we define $R_{yz}(\tau)=E[y(t)z(t+\tau)]$, where $y(t)$ and $z(t)$ are two real processes. Then it is easy to verify [24]

$$\begin{aligned}
&E[y(t)z'(t+\tau)]=\dot{R}_{yz}(\tau),\\
&E[z(t)y'(t+\tau)]=\dot{R}_{zy}(\tau)=\dot{R}_{yz}(-\tau),\\
&E[y'(t)z'(t+\tau)]=-\ddot{R}_{yz}(\tau),
\end{aligned}\tag{7}$$

where dot denotes differentiation with respect to τ. Based on (7), we build $\boldsymbol{\Sigma}_{12}$ and $\boldsymbol{\Sigma}_{22}$, antisymmetric and symmetric matrices, respectively, as follows

$$\begin{aligned}
\boldsymbol{\Sigma}_{12}&=\tfrac{1}{2}\begin{bmatrix}\mathrm{Re}[\dot{\xi}] & \mathrm{Re}[\dot{\zeta}] & -\mathrm{Im}[\dot{\xi}] & -\mathrm{Im}[\dot{\zeta}]\\ -\mathrm{Re}[\dot{\zeta}] & \mathrm{Re}[\dot{\xi}] & -\mathrm{Im}[\dot{\zeta}] & -\mathrm{Im}[\dot{\xi}]\\ \mathrm{Im}[\dot{\xi}] & \mathrm{Im}[\dot{\zeta}] & \mathrm{Re}[\dot{\xi}] & \mathrm{Re}[\dot{\zeta}]\\ \mathrm{Im}[\dot{\zeta}] & \mathrm{Im}[\dot{\xi}] & -\mathrm{Re}[\dot{\zeta}] & \mathrm{Re}[\dot{\xi}]\end{bmatrix},\\
\boldsymbol{\Sigma}_{22}&=\tfrac{1}{2}\begin{bmatrix}-\mathrm{Re}[\ddot{\xi}] & -\mathrm{Re}[\ddot{\zeta}] & \mathrm{Im}[\ddot{\xi}] & \mathrm{Im}[\ddot{\zeta}]\\ -\mathrm{Re}[\ddot{\zeta}] & -\mathrm{Re}[\ddot{\xi}] & -\mathrm{Im}[\ddot{\zeta}] & \mathrm{Im}[\ddot{\xi}]\\ \mathrm{Im}[\ddot{\xi}] & -\mathrm{Im}[\ddot{\zeta}] & -\mathrm{Re}[\ddot{\xi}] & -\mathrm{Re}[\ddot{\zeta}]\\ \mathrm{Im}[\ddot{\zeta}] & \mathrm{Im}[\ddot{\xi}] & -\mathrm{Re}[\ddot{\zeta}] & -\mathrm{Re}[\ddot{\xi}]\end{bmatrix},
\end{aligned}\tag{8}$$

in which we have used the shorthand notations $\dot{\xi}=\dot{\rho}_{11,11}(0)$, $\dot{\zeta}=\dot{\rho}_{11,12}(0)$, $\ddot{\xi}=\ddot{\rho}_{11,11}(0)$, and $\ddot{\zeta}=\ddot{\rho}_{11,12}(0)$.

In our numerical example, we use the macrocell space-time correlation model of [9]. We choose macrocells because the correlation among subchannels is particularly high within macrocells, where the angle spread at the elevated base station (BS) is normally small, say, less than 10 degrees (see references in [9]), and the distribution of angle of arrival (AOA) at the mobile station (MS) could be far from uniform [27] [28]. Both of these induce high nonnegligible correlations. For a 2×1 Rayleigh channel, Eq. (12) of [9] yields these correlations

$$\begin{aligned}
&\rho_{11,11}(\tau)=[I_0(\kappa)]^{-1}I_0\left(\left\{\kappa^2-4\pi^2f_D^2\tau^2-j\,4\pi\kappa\cos(\gamma_0-\mu)\,f_D\tau\right\}^{1/2}\right),\\
&\rho_{11,12}(\tau)=[I_0(\kappa)]^{-1}\\
&\quad\times e^{j\cos(\alpha)2\pi\delta/\lambda}I_0\Big(\big\{\kappa^2-4\pi^2f_D^2\tau^2-4\pi^2(\delta/\lambda)^2\Delta^2\sin^2(\alpha)\\
&\quad+8\pi^2(\delta/\lambda)f_D\tau\,\Delta\sin(\alpha)\sin(\gamma_0)\\
&\quad-j2\kappa\left[2\pi f_D\tau\cos(\mu-\gamma_0)-2\pi(\delta/\lambda)\Delta\sin(\alpha)\sin(\mu)\right]\big\}^{1/2}\Big),
\end{aligned}\tag{9}$$

where $I_0(.)$ is the zero-order modified Bessel function, $\kappa\ge 0$ controls the angle spread at the MS, $\mu\in[-\pi,\pi)$ accounts for the mean direction of AOA at the MS, γ_0 is the direction of the motion

of MS (not to be confused with SNR in this paper), f_D denotes the maximum Doppler shift, α represents the direction of the BS array, λ is the wavelength, δ stands for the element spacing at the BS, and finally 2Δ is the spread of the angle of departure from the BS.

Consider the transmit BS array, where the two elements are spaced by δ, is perpendicular to the horizontal *x* axis, $\alpha = 90^o$, and the receive single MS antenna is moving on the *x* axis, towards the transmit array, $\gamma_0 = 180^o$, with a constant speed such $f_D = 20$ Hz. The angle spread at the BS is $2\Delta = 4^o$, whereas at the MS is 66^o, equivalent to $\kappa = 3$, around the mean AOA of $\mu = 36^o$ at the MS. The values of κ and μ are estimated from measured data [27]. In Fig. 1 and Fig. 2 we have plotted the DCR and AFD of $\gamma(t)$ with respect to the threshold γ_{th}, obtained via (3) and (5) divided by (3), respectively, as a function of the normalized power threshold $\gamma_{th}/\overline{\gamma}_{11}$. In both figures, two BS element spacings of $\delta = \lambda$ and 5λ are considered, which correspond, respectively, to these spatial correlations: $|\zeta| = |\rho_{11,12}(0)| = 0.995$ and 0.886. Close agreement between the simulation results, given in both figures for $\delta = 5\lambda$, and the theoretical curves verifies the accuracy of the analytic calculations. The spatio-temporally correlated MIMO channel is simulated using the spectral representation method [29].

Also in Fig. 1 and Fig. 2 we have plotted the DCR and AFD if we ignore the spatial correlation, i.e., incorrect assumption of independent subchannels $h_{11}(t)$ and $h_{12}(t)$. To do this, we have used Eqs. (15) and (17) of [20], which after minor corrections result in

$$\mathrm{DCR}\{\gamma(t),\gamma_{th}\} = \frac{1}{\sqrt{\pi}}\left(\frac{\gamma_{th}}{\overline{\gamma}_{11}}\right)^{3/2}\exp\left(\frac{-\gamma_{th}}{\overline{\gamma}_{11}}\right)\left(\frac{b_2}{b_0}-\frac{b_1^2}{b_0^2}\right)^{1/2}, \quad (10)$$

$$\mathrm{AFD}\{\gamma(\mathrm{t}),\gamma_{th}\} = \frac{\sqrt{\pi}\left[\exp\left(\gamma_{th}/\overline{\gamma}_{11}\right)-1-\left(\gamma_{th}/\overline{\gamma}_{11}\right)\right]}{\left(\gamma_{th}/\overline{\gamma}_{11}\right)^{3/2}}\left(\frac{b_2}{b_0}-\frac{b_1^2}{b_0^2}\right)^{-1/2}, \quad (11)$$

$$\begin{aligned} b_1/b_0 &= 2\pi f_D\cos(\mu)I_1(\kappa)[I_0(\kappa)]^{-1}, \\ b_2/b_0 &= 2\pi^2 f_D^2[I_0(\kappa)+I_2(\kappa)\cos(2\mu)][I_0(\kappa)]^{-1}. \end{aligned} \quad (12)$$

Note that b_1/b_0 and b_2/b_0 in (12) have been calculated according to $\rho_{11,11}(\tau)$ in (9), whereas $\rho_{11,12}(\tau) \equiv 0$ due to neglecting the existing spatial correlation. As Fig. 1 shows, high spatial correlations introduce large deviations from the case where there is no correlation between the two subchannels. On the other hand, according to Fig. 2, AFD increases as the spatial correlation increases. This was expected since the correlation reduces the amount of diversity. As a numerical example, to have an AFD of 10 msec. below a fixed threshold, one needs a 2.6 dB increase in $\overline{\gamma}_{11} = E_s/N_0$, the average received SNR per symbol over each subchannel, for a spatial correlation of 0.995. This increase for the 0.886 spatial correlation is 2 dB.

C. Application of Scalar ASD to Adaptive Modulation

In adaptive modulation schemes for MIMO channels, the total received (post-processing) SNR is a good measure of channel quality as it captures the impacts of many parameters involved such as the space-time coding/decoding used, constellation size/shape, antenna correlations and polarizations, etc. [17]. The entire range of total received SNR, $[0,\infty]$, needs to be discretized into $k+1$ regions $[0,\gamma_1]$, $[\gamma_1,\gamma_2]$, …, $[\gamma_{k-1},\gamma_k]$, and $[\gamma_k,\infty]$. The ASD of each individual region can be used to determine, for example, the tradeoff between power/rate adaptation policies and the number of regions, as well as the thresholds $\{\gamma_1,\gamma_2,...,\gamma_k\}$.

D. Application of Scalar ASD to Markov Modeling

There is a growing interest in representing fading channels with finite state Markov models [8] [30]-[32] as they significantly facilitate the performance analysis of complex communication protocols over channels with memory. Development of a Markov model for MIMO fading channels can be done using the approach taken for receive diversity combiners [15], i.e., partitioning the entire range of total received SNR, and treating each subregion as a state. The transition probability of $\gamma(t)$ from one state to another can be determined using the ICR of $\gamma(t)$. The ASD of $\gamma(t)$ can be employed for choosing the thresholds in order to obtain, for example, an equal-duration partitioning, or other types of partitioning.

III. Vector Crossing in MIMO Systems

Here first we formulate the problem and discuss the solution. Since the solution in the most general case is rather complicated, we consider a special situation and then apply it to two cases of interest.

A. Mathematical Formulation

Consider a time-selective narrowband $M \times N$ matrix channel, composed of *MN* complex zero-mean Gaussian processes, correlated in both space and time. Obviously the envelope of subchannels are Rayleigh distributed. As before, $h_{lp}(t)$ denotes the complex gain of the subchannel connecting the *p*-th transmitter to the *l*-th receiver. Suppose at $t = t_0$, all the subchannel gains are observed. Now we need to determine for how long, in average, the maximum absolute deviation of all the *MN* processes from their observed values at $t = t_0$, simultaneously, does not exceed a certain bound ε. In other words, starting at $t = t_0$, this is the average time over which $|\mathrm{Re}[h_{lp}(t)] - \mathrm{Re}[h_{lp}(t_0)]| < \varepsilon$ and $|\mathrm{Im}[h_{lp}(t)] - \mathrm{Im}[h_{lp}(t_0)]| < \varepsilon$, for all *l*'s and *p*'s. Mathematically speaking, this is equivalent to the average stay time of a vector Gaussian process consisting of $2MN$ real correlated processes, within a hypercube with equal sides of length 2ε. For $M = N = 1$, a SISO channel, the idea is depicted in Fig. 3, where T_{stay} is the stay time of the real and imaginary parts of $h_{11}(t)$ within the 2ε-square, centered on the process at $t = t_0$. Obviously we are interested in calculating $E[T_{stay}]$, the ASD.

To compute this vector ASD, similar to the scalar ASD of the previous section, we need to divide the probability of falling this Gaussian vector into the 2ε-hypercube, by the associated outcrossing rate (OCR) of the vector process. For the numerator, many techniques are available [33], whereas the OCR can be derived from Eq. (3.1) of [34], in the form of a multidimensional surface integral (one can also derive (3) from Eq. (3.1) of [34]). More specifically, let $\mathbf{H}(t)$ represents the $M \times N$ matrix channel. Also let $\mathbf{h}_{re}(t) = \mathrm{vec}(\mathrm{Re}[\mathbf{H}(t)])$ and $\mathbf{h}_{im}(t) = \mathrm{vec}(\mathrm{Im}[\mathbf{H}(t)])$, two $MN \times 1$ real vectors, where vec(.) gives a column vector, constructed by stacking the columns of its matrix argument. The ASD of the $2MN \times 1$ real vector process $\mathbf{h}(t) = [\mathbf{h}_{re}^T(t)\ \mathbf{h}_{im}^T(t)]^T$ within the hypercube of side 2ε, centered at $\mathbf{h}(t_0)$, $HC[\mathbf{h}(t_0), 2\varepsilon]$, is given by

$$\mathrm{ASD}\{\mathbf{h}(\mathrm{t}), HC[\mathbf{h}(t_0), 2\varepsilon]\} = \frac{\Pr[\mathbf{h}(\mathrm{t}) \in HC[\mathbf{h}(t_0), 2\varepsilon]]}{\mathrm{OCR}\{\mathbf{h}(\mathrm{t}), HC[\mathbf{h}(t_0), 2\varepsilon]\}}. \quad (13)$$

B. Special Case of Isotropic Scattering and No Spatial Correlation

To come up with a simple solution for (13) to obtain some intuition, we assume there is no spatial correlation between the *MN* subchannels. We further assume isotropic scattering, i.e., uniform distribution of AOA at the receiver, which entails Clarke's correlation $2J_0(2\pi f_D \tau)$ for each individual complex subchannel, where $J_0(.)$ is the zero-order Bessel function. Under theses conditions it is easy to verify that all the elements of $\mathbf{h}(t)$ are independent processes, with zero mean and unit variance. Let $\mathbf{h}(t_0) = \theta\mathbf{1}$, where θ is a real number and $\mathbf{1}$ is an all one vector. Obviously we are looking at the

case where at time t_0, the real and imaginary parts of all the subchannels have taken the same value θ. It is easy to show that the numerator of (13) is given by $[\Phi(\theta+\varepsilon)-\Phi(\theta-\varepsilon)]^{2MN}$. We derive the denominator from Eq. (19) of [35], also possible to derive from Eq. (3.1) of [34], as $2\sqrt{2}MNf_D \exp[-(\theta^2+\varepsilon^2)/2]\cosh(\theta\varepsilon)[\Phi(\theta+\varepsilon)-\Phi(\theta-\varepsilon)]^{2MN-1}$, where cosh(.) is the hyperbolic cosine. This gives us

$$\mathrm{ASD}\{\mathbf{h}(t),HC[\theta\mathbf{1},2\varepsilon]\}=\frac{[\Phi(\theta+\varepsilon)-\Phi(\theta-\varepsilon)]\exp[(\theta^2+\varepsilon^2)/2]}{2\sqrt{2}MNf_D\cosh(\theta\varepsilon)}. \quad (14)$$

C. Application: Analysis of the Block Fading Model

In many wireless communication scenarios, due to the low mobility of the users and also the quasi-stationarity of the environment, it is common to assume that the channel remains constant over a long block of symbols, and then jumps to another random constant for the next block. This gives rise to the so-called block fading model [36], which has been used extensively for coding/information-theoretic studies in fading channels [37]. Besides the physical motivation just described, this piecewise-constant approximation of the continuously time-varying random fading facilitates the theoretical analysis [38]. The block fading model also appears in the context of differential detection schemes, which are devised to bypass the channel estimation at the receiver [39] [40]. However, error floors appear at high SNR when the time-varying nature of the channel dominates, i.e., the piecewise-constant approximation of block fading model becomes less accurate [41] [42], which in turn degrades the performance of the associated designs. So, in general, it is important to quantify the conditions under which the block fading model is a reasonable approximation to the continuously varying MIMO fading channel.

For $M=N$, the normalized ASD, $f_D\,\mathrm{ASD}\{\mathbf{h}(t),HC[\theta\mathbf{1},2\varepsilon]\}$, is plotted in Fig. 4 with respect to θ, with ε as a parameter. Some simulation results are also included, to verify the theory. Interestingly, for any fixed ε, ASD decreases as M increases. This means that the block fading model remains accurate for a shorter period, as the number of transmitters and/or receivers increases. On the other hand, when M is fixed, ASD decreases as ε decreases. This was expected as it should take less time for a vector process to exit a small region than a large one. Finally we note that for any M and ε, ASD decreases when θ increases. This implies that the zero-mean vector Gaussian process tends to stay more often around small values, rather than large values.

D. Application: Vector AFD in MIMO Channels

In the numerical example of Subsection II.B, we focused on the scalar AFD in MIMO channels, where the AFD was defined for the total instantaneous received SNR per symbol, $\gamma(t)\propto\sum_{l,p}|h_{lp}(t)|^2$, a scalar process. Now we define the vector AFD as the average stay duration inside a hypercube with equal sides of size 2ε, centered at the origin, i.e., $\theta=0$. Then Eq. (14) gives the vector AFD as $(2\sqrt{2}MNf_D)^{-1}[1-2\Phi(-\varepsilon)]\exp(\varepsilon^2/2)$. Obviously the vector AFD tends to zero and infinity as $\varepsilon\to 0$ and ∞, respectively.

IV. Conclusion

The concepts of level crossing rate (LCR) and average fade duration (AFD) are well understood for single-input single-output fading channels. However, apparently they have not been studied so far, in the context of multiple-input multiple-output (MIMO) channels. In this paper have looked at a variety of possible approaches and definitions for MIMO LCR and AFD. When feasible, closed-from solutions are provided, and illustrated by numerical examples and simulations. Applications of MIMO LCR and AFD to adaptive modulation in MIMO channels, Markov modeling, and block fading approximation of MIMO channels are discussed as well.

References

[1] J. F. DeRose, *The Wireless Data Handbook*, fourth ed., New York: Wiley, 1999.

[2] E. Biglieri, D. Divsalar, P. J. McLane, and M. K. Siomn, *Introduction to Trellis-Coded Modulation with Applications*. New York: Macmillan, 1991.

[3] K. Y. Tsie, P. Fines, and A. H. Aghvami, "Concatenated trellis-coded 8-ary PSK for land mobile satellite communications," in *Proc. IEEE Int. Conf. Commun.*, Chicago, IL, 1992, pp. 778-782.

[4] A. J. Goldsmith and S. G. Chua, "Adaptive coded modulation for fading channels", *IEEE Trans. Commun.*, vol. 46, pp. 595-602, 1998.

[5] J. P. Linnartz, *Narrowband Land-Mobile Radio Networks*. Boston, MA: Artech House, 1993.

[6] L. Yang and M. S. Alouini, "Average outage duration of multiuser wireless communication systems with a minimum signal power requirement," in *Proc. IEEE Vehic. Technol. Conf.*, Birmingham, AL, 2002, pp. 1507-1511.

[7] L. F. Chang, "throughput estimation of ARQ protocols for a Rayleigh fading channel using fade- and interfade-duration statistics," *IEEE Trans. Vehic. Technol.*, vol. 40, pp. 223-229, 1991.

[8] H. S. Wang and N. Moayeri, "Finite-state Markov channel-a useful model for radio communication channels," *IEEE Trans. Vehic. Technol.*, vol. 44, pp. 163-171, 1995.

[9] A. Abdi and M. Kaveh, "A space-time correlation model for multielement antenna systems in mobile fading channels," *IEEE J. Select. Areas Commun.*, vol. 20, pp. 550-560, 2002.

[10] Z. Latinovic, A. Abdi, and Y. Bar-Ness, "A wideband space-time model for MIMO mobile fading channels," in *Proc. IEEE Wireless Commun. Networking Conf.*, New Orleans, LA, 2003, pp. 338-342.

[11] A. Abdi and M. Kaveh, "Level crossing rate in terms of the characteristic function: A new approach for calculating the fading rate in diversity systems," *IEEE Trans. Commun.*, vol. 50, pp. 1397-1400, 2002.

[12] A. Abdi, W. C. Lau, M. S. Alouini, and M. Kaveh, "A new simple model for land mobile satellite channels: First- and second-order statistics," *IEEE Trans. Wireless Commun.*, vol. 2, pp. 519-528, 2003.

[13] M. D. Yacoub, C. R. C. M. da Silva, and J. E. Vargas Bautista, "Second-order statistics for diversity-combining techniques in Nakagami-fading channels," *IEEE Trans. Vehic. Technol.*, vol. 50, pp. 1464-1470, 2001.

[14] C. D. Iskander and p. T. Mathiopoulos, "Analytical level crossing rates and average fade durations for diversity techniques in Nakagami fading channels," *IEEE Trans. Commun.*, vol. 50, pp. 1301-1309, 2002.

[15] W. Tang and S. A. Kassam, "Finite-state Markov models for correlated Rayleigh fading channels," in *Proc. Conf. Inform. Sci. Syst.*, Princeton University, Princeton, NJ, 2002, pp. 404-409.

[16] R. W. Heath, Jr., and A. J. Paulraj, "Characterization of MIMO channels for spatial multiplexing systems," in *Proc. IEEE Int. Conf. Commun.*, Helsinki, Finland, 2001, pp. 591-595.

[17] S. Catreux, V. Erceg, D. Gesbert, and R. W. Heath, "Adaptive modulation and MIMO coding for broadband wireless data networks," *IEEE Commun. Mag.*, vol. 40, no. 6, pp. 108-115, 2002.

[18] P. Stoica and G. Ganesan, "Maximum-SNR space-time designs for MIMO channels," in *Proc. IEEE Int. Conf. Acoust., Speech, Signal Processing*, Salt Lake City, UT, 2001, pp. 2425-2428.

[19] G. Ganesan and P. Stoica, "Space-time block codes: a maximum SNR approach," *IEEE Trans. Inform. Theory*, vol. 47, pp. 1650-1656, 2001.

[20] Y. C. Ko, A. Abdi, M. S. Alouini, and M. Kaveh, "A general framework for the calculation of the average outage duration of diversity systems over generalized fading channels," *IEEE Trans. Vehic. Technol.*, vol. 51, pp. 1672-1680, 2002.

[21] A. M. Hasofer, "The upcrossing rate of a class of stochastic processes," in *Studies in Probability and Statistics*. E. J. Williams, Ed., New York: North-Holland, 1974, pp. 153-159.

[22] G. Lindgren, "Slepian models for χ^2–processes with dependent components with application to envelope upcrossings," *J. Appl. Prob.*, vol. 26, pp. 36-49, 1989.

[23] W. C. Y. Lee, *Mobile Communications Engineering: Theory and Applications*, 2nd ed., New York: McGraw-Hill, 1998.

[24] A. Papoulis, *Probability, Random Variables, and Stochastic Processes*, 3rd ed., Singapore: McGraw-Hill, 1991.

[25] B. Picinbono, "On circularity," *IEEE Trans. Signal Processing*, vol. 42, pp. 3473-3482, 1994.

[26] F. D. Neeser and J. L. Massey, "Proper complex random processes with applications to information theory," *IEEE Trans. Inform. Theory*, vol. 39, pp. 1293-1302, 1993.

[27] A. Abdi, J. A. Barger, and M. Kaveh, "A parametric model for the distribution of the angle of arrival and the associated correlation function and power spectrum at the mobile station," *IEEE Trans. Vehic. Technol.*, vol. 51, pp. 425-434, 2002.

[28] H. Xu, M. Gans, D. Chizhik, J. Ling, P. Wolniansky, and R. Valenzuela, "Spatial and temporal variations of MIMO channels and impacts on capacity," in *Proc. IEEE Int. Conf. Commun.*, New York, 2002, pp. 262-266.

[29] K. Acolatse and A. Abdi, "Efficient simulation of space-time correlated MIMO mobile fading channels," to be published in *Proc. IEEE Vehic. Technol. Conf.*, Orlando, FL, 2003.

[30] W. Turin and R. van Nobelen, "Hidden Markov modeling of flat fading channels," *IEEE J. Select. Areas Commun.*, vol. 16, pp. 1809-1817, 1998.

[31] Q. Zhang and S. A. Kassam, "Finite-state Markov model for Rayleigh fading channels," *IEEE Trans. Commun.*, vol. 47, pp. 1688-1692, 1999.

[32] M. J. Chu, D. L. Goeckel, and W. E. Stark, "On the design of Markov models for fading channels," in *Proc. IEEE Vehic. Technol. Conf.*, Amsterdam, the Netherlands, 1999, pp. 2372-2376.

[33] S. S. Gupta, "Bibliography on the multivariate normal integrals and related topics," *Ann. Math. Statist.*, vol. 34, pp. 829-838, 1963.

[34] R. Illsley, "The excursions of a stationary Gaussian process outside a large two-dimensional region," *Adv. Appl. Prob.*, vol. 33, pp. 141-159, 2001.

[35] D. Veneziano, M. Grigoriu, and C. A. Cornell, "Vector-process models for system reliability," *ASCE J. Eng. Mech. Div.*, vol. 103, pp. 441-460, 1977.

[36] E. Biglieri, G. Caire, and G. Taricco, "Coding and modulation under power constraints," *IEEE Pers. Commun. Mag.*, vol. 5, no. 3, pp. 32-39, 1998.

[37] E. Biglieri, J. Proakis, and S. Shamai, "Fading channels: Information-theoretic and communication aspects," *IEEE Trans. Inform. Theory*, vol. 44, pp. 2619-2692, 1998.

[38] G. Kaplan and S. Shamai, "Achievable performance over the correlated Rician channel," *IEEE Trans. Commun.*, vol. 42, pp. 2967-2978, 1994.

[39] H. Jafarkhani and V. Tarokh, "Multiple transmit antenna differential detection from generalized orthogonal designs," *IEEE Trans. Inform. Theory*, vol. 47, pp. 2626-2631, 2001.

[40] B. L. Hughes, "Differential space-time modulation," *IEEE Trans. Inform. Theory*, vol. 46, pp. 2567-2578, 2000.

[41] C. B. Peel and A. L. Swindlehurst, "Performance of unitary space-time modulation in a continuously changing channel," in *Proc. IEEE Int. Conf. Commun.*, Helsinki, Finland, 2001, pp. 2805-2808.

[42] B. Bhukania and P. Schniter, "Multiple-symbol detection of differential unitary space-time modulation in fast-fading channels with known correlation," in *Proc. Conf. Inform. Sci. Syst.*, Princeton University, Princeton, NJ, 2002, pp. 248-253.

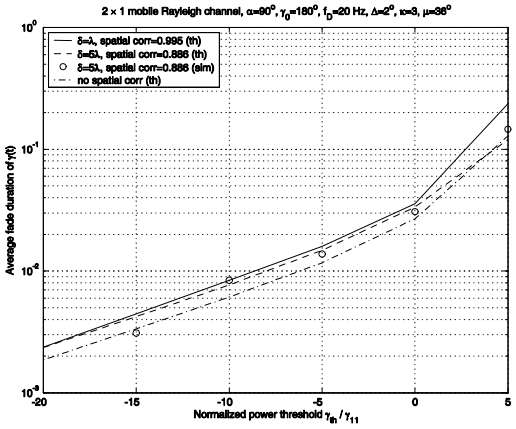

Fig. 2. Average fade duration of total instantaneous SNR in a 2×1 channel, with and without spatial correlation (th: theory, sim: simulation).

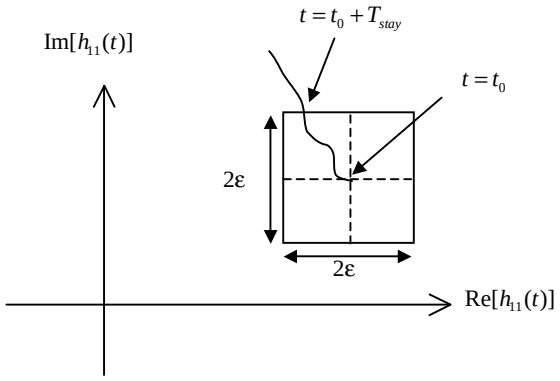

Fig. 3. Graphical representation of the concept of the stay duration of a single complex process, a SISO channel, within a square region.

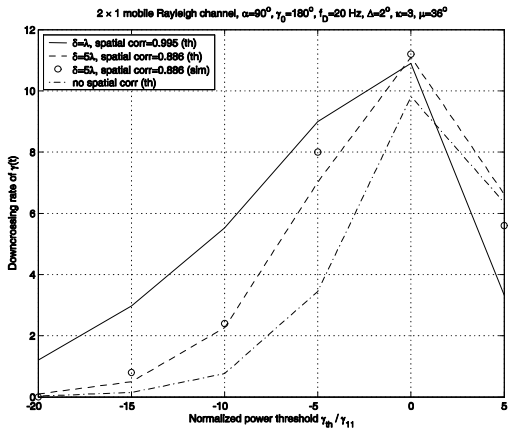

Fig. 1. Downcrossing rate of total instantaneous SNR in a 2×1 channel, with and without spatial correlation (th: theory, sim: simulation).

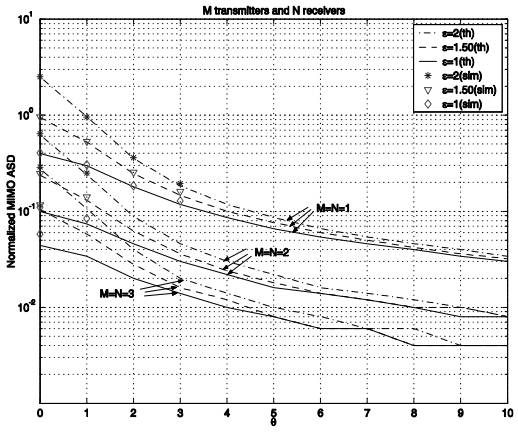

Fig. 4. Normalized average stay duration in a MIMO channel with the same number of transmit and receive antennas (th: theory, sim: simulation).